

Analytical Investigation on Some K X-Ray Fluorescence Parameters of Barium Compounds

B. GÖKER DURDU^{a,*}, E. AKKUTLU^b,
A. KÜÇÜKÖNDER^{c,d} AND H. ÇAM^e

^a*Kilis 7 Aralık University, Vocational School of Health Services, Opticianry Program, Karataş Campus, 79000, Kilis-Turkey*

^b*Kilis 7 Aralık University, The Institute for Graduate Studies in Science and Engineering, Department of Physics, Karataş Campus, 79000, Kilis-Turkey*

^c*Kahramanmaraş Sütcü Imam University, Faculty of Science and Letters, Department of Physics, Aşağı Campus, 46100, K. Maraş-Turkey*

^d*Kahramanmaraş İstiklal University Rectorate, Cumhuriyet Street 7, 46100, K. Maraş-Turkey*

^e*Kahramanmaraş Sütcü Imam University, Vocational School of Technical Sciences, Electronic Technology Program, Aşağı Campus, 46100, K. Maraş-Turkey*

Received: 19.10.2021 & Accepted: 24.01.2022

Doi: [10.12693/APhysPolA.141.474](https://doi.org/10.12693/APhysPolA.141.474)

*e-mail: bgoker@hotmail.com

Fluorescence cross-sections ($\sigma_{K\alpha}$, $\sigma_{K\beta}$, σ_{total}), K_{β}/K_{α} X-ray intensity ratios, probabilities of the vacancy transfer from K to L shell (η_{KL}), and Auger electrons emission ratios for Ba compounds were studied using K_i ($i = \alpha, \beta$) X-rays line intensities. The samples were excited by γ -rays 59.5 keV produced by the ²⁴¹Am radioisotope source. The K X-rays emitted from the samples were detected with a high resolution Si(Li) detector. The experimental results were compared with other theoretical and experimental values of Ba compounds.

topics: X-ray fluorescence, intensity ratio, K shell fluorescence yield, vacancy transfer probabilities

1. Introduction

It is well known that the chemical combination and the physical properties of atoms have an effect on X-ray emission spectra. The changes of the X-ray fluorescence parameters of elements in chemical compounds can be explained as a result of changes in the valance electron configurations or the charge transfer effect due to the presence of alien elements. Measurements of the K and L shell fluorescence parameters are important for the development of more reliable theoretical models describing fundamental ionization phenomena, because comparison of experimental values of X-rays with the calculated theoretical values provide a check on the validity of various physical parameters such as X-ray emission rate, fluorescence yields, photoionization cross-sections. For this reason, the chemical effects on the X-ray fluorescence parameters of elements and their compounds were investigated and interpreted by several research groups using chemical bonding type, valance band structure, oxidation number, and symmetry. In various compounds, especially for unpaired electrons, there are different bond distances, binding energies and the probability

of ejection Auger electrons. Changes in these parameters cause different interactions between the ligand and the central atom [1].

In recent decades, chemical effects on the K shell X-ray fluorescence parameters have been studied by many researchers. Turhan et al. [2] measured the chemical effect on K shell X-ray fluorescence parameters for some Mn and Ni compounds. Uğurlu and Demir [3] investigated the K X-ray fluorescence (XRF) parameters, namely the fluorescence cross-section, the vacancy transfer probabilities and fluorescence yield of some fourth-period elements in an external magnetic field (8000 Gauss) [3]. The L X-ray fluorescence cross-sections for Ba, La and Ce at 7, 8, 9 and 10 keV synchrotron radiation was studied by Kumar et al. [4]. The $K \rightarrow L_i$ ($i = 2, 3$), $K \rightarrow L$, and $K \rightarrow M$ shell vacancy transfer probabilities for La, Ce, Pr, Nd, Sm, Eu, Gd, Tb, Dy and Er at 59.54 keV using a reflection geometry were determined by Akman [5]. Akman also determined the $K \rightarrow L$ shell vacancy transfer probabilities for some elements in the atomic range $30 \leq Z \leq 58$, using the semi-empirical values of K shell fluorescence yield and the experimental values of K_{β}/K_{α} X-Ray intensity ratio. Furthermore, the KLX/KLL and

KXY/KLL Auger electrons emission ratios for the same elements were obtained using the experimental values of K_β/K_α X-ray intensity ratio [6]. The $K \rightarrow L$ shell total vacancy transfer probabilities of low Z elements, Co, Ni, Cu, and Zn, measuring the K_β/K_α intensity ratio adopting 2π -geometry were analyzed by Anand et al. [7]. The K shell fluorescence yields, $K \rightarrow L$ shell vacancy transfer probabilities and K_β/K_α X-ray intensity ratios for Cr, Cu, Zn, and their compounds using synchrotron radiation were obtained by Mirji et al. [8]. Chemical effects on K_α , K_β X-ray production cross-sections and K_β/K_α X-ray intensity ratios for Co, Ni, Cu and Zn elements in the phthalocyanine complexes were studied by Doğan et al. [9], and the results were interpreted according to the charge transfer process. The K -shell X-ray intensity ratios, radiative and total vacancy transfer probabilities of platinum, gold and lead by employing the 2π -geometrical configuration and the weak γ -source were measured by Anand et al. [10]. Chemical sensitivities of the K shell fluorescence K_β/K_α X-ray intensity ratios yields, the $K \rightarrow L$ shell vacancy transfer probabilities for some selected cerium compounds using the 59.54 keV energy of photons emitted from a 5 mCi ^{241}Am radioactive source were studied by Tursucu and Demir [11]. The K shell intensity ratios K_β/K_α for 9 elements in the atomic range $40 \leq Z \leq 50$ using a weak ^{133}Ba γ -source at an excitation energy of 80.997 keV were determined by Tursucu et al. [12]. Probabilities for the vacancy transfer from the $K \rightarrow L$ shell (η_{KL}) for eleven high atomic number elements using the measured K and L shells X-ray cross-sections at 123.6 keV, were measured by Apaydın and Tirasoglu [13].

Recently, the K and L X-rays fluorescence cross-sections, X-rays intensity ratios, average L shell fluorescence yields, ratios of emission probabilities of Auger electrons ($u = p(KLX)/p(KLL)$, $\nu = p(KXY)/p(KLL)$) and the vacancy transfer probabilities for some elements and compounds were determined by our research group [14–16].

Although the vacancy transfer probabilities have been studied by some authors, none of the studies have addressed the chemical effects on the vacancy transfer probabilities. In the present study, ratios of emission probabilities of Auger electrons and the vacancy transfer probability from the K to L shell for barium compounds were determined experimentally using K_i X-rays line intensity ($i = \alpha, \beta$). These effects are interpreted in terms of the valence electron distribution and chemical bonding. It is the first analytical investigation of emission probabilities of Auger electrons and the vacancy transfer probabilities for Ba compounds.

Barium plays a key role in the production of many products in the industry. Barium sulfate (BaSO_4) has γ and X-ray emission (radiopaque) and is used in the medical sector for X-ray applications, e.g. cancer diagnosis. It is also a compound used in paper coatings, batteries and plastic products and

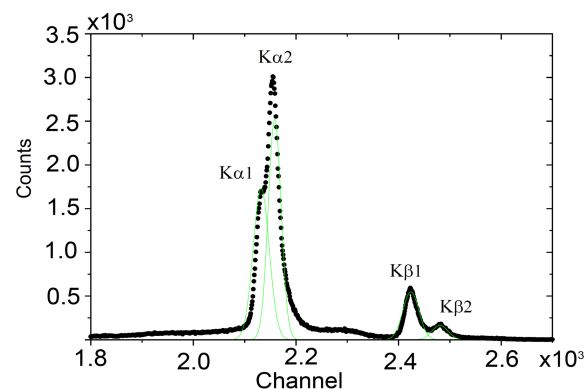


Fig. 1. Characteristic K X-ray emission spectra of barium.

textile products. It is used as a whitening pigment and thinner in the production of oil painting. Barium carbonate (BaCO_3), another common barium compound, is used in the manufacture of ceramics and some types of glass. It is a component in clay slurries used in drilling oil wells. Barium carbonate is also used to purify some chemical solutions and is the primary base material for the manufacture of other barium compounds. Barium oxide (BaO) is one of the compounds used in the removal of water from solvents and in the petroleum industry. Barium nitrate ($\text{Ba}(\text{NO}_3)_2$) is used in fireworks and ceramic glazes because it gives green flames. Barium chloride (BaCl) is used as a water softener. Barium oxide (BaO) absorbs moisture easily and is used as a desiccant. Barium peroxide (BaO_2) forms hydrogen peroxide (H_2O_2) when it is mixed with water and is used as a bleaching agent that activates when wet [17].

2. Experimental procedure

The geometry of the experimental set-up was given in our earlier paper [15]. The purity of commercially obtained materials was better than 99%. To reduce the particle size effect, the powder samples were sieved with a 400 mesh and supported on a mylar films. The samples were excited by using the heavily filtered 59.5 keV γ -photons emitted from the 75 mCi ^{241}Am radiative source, X-rays emitted from samples were detected by a Si(Li) (FWHM 155 eV at 5.9 keV) detector system. Two typical K X-ray spectra obtained from barium is given in Fig. 1.

3. Data analysis procedure

3.1. Determination of detector efficiency

The values of detection efficiency $I_o G \epsilon_{K_i}$ in the present experimental geometry were determined in a separate experiment in the same geometry, the K X-ray spectra of samples in the atomic

range $19 \leq Z \leq 57$ were used. The effective overall detection efficiency for the present geometry was determined by the following relation

$$I_0 G \varepsilon_{K_i} = \frac{N_{K_i}}{\sigma_{K_i} \beta_{K_i} t}, \quad i = \alpha, \beta. \quad (1)$$

Here, N_{K_i} is the number of counts under photo peak corresponding to K_i X-ray of element of interest, σ_{K_i} is the theoretical fluorescence cross-sections, β_{K_i} is the self-absorption correction factor, t is the mass per unit area of the sample [g/cm^2].

The self-absorption correction factor was calculated from

$$\beta_{K_i} = \frac{1 - \exp \left[- \left(\frac{\mu_{\text{inc}}}{\cos(\phi_1)} + \frac{\mu_{K_i}}{\cos(\phi_2)} \right) t \right]}{\left(\mu_{\text{inc}} \cos(\phi_1) + \mu_{K_i} \cos(\phi_2) \right) t}, \quad (2)$$

where μ_{inc} and μ_{K_i} are the mass absorption coefficients of the incident photons and the emitted K_i X-rays [18], respectively. The angle of photon incidence is ϕ_1 , and the angle of emitted characteristic X-ray from the sample is ϕ_2 with respect to the normal to the sample surface.

Theoretical fluorescence cross-sections can be computed using

$$\sigma_{K_i} = \sigma_K(E) \omega_K F_{K_i}, \quad (3)$$

where $\sigma_K(E)$ represents the K -shell photoionization cross-section obtained from Scofield [19] for samples at related energy E , ω_K represents the K -shell fluorescence yield taken from Krause [20]. The quantities, F_{K_α} and F_{K_β} , represent the K_α and K_β fractional X-ray emission rates and are defined as

$$F_{K_\alpha} = \left(1 + \frac{I_{K_\beta}}{I_{K_\alpha}} \right)^{-1} \quad (4)$$

and

$$F_{K_\beta} = \left(1 + \frac{I_{K_\alpha}}{I_{K_\beta}} \right)^{-1}, \quad (5)$$

where intensity ratio I_{K_β}/I_{K_α} is taken from Scofield [21]. The results of $I_0 G \varepsilon$ are shown in Fig. 2 as a functions of the average K_i ($i = \alpha, \beta$) X-ray energy [keV].

3.2. Determination of K X-ray production cross-section, intensity ratio and fluorescence yield

Experimental K_i X-ray fluorescence cross-sections for Ba compounds were evaluated using the relation

$$\sigma_{K_i} = \frac{N_{K_i}}{\varepsilon_{K_i} \beta_{K_i} t I_0 G} \quad (6)$$

for $i = \alpha, \beta$, where N_{K_i} is the number of counts under the K_i X-ray photo peak, I_0 is the intensity of exciting radiation, G is the geometry factor, ε_{K_i} is the detector efficiency for K_i X-rays, t is mass per unit area of the sample [g/cm^2] and β_{K_i} is the self-absorption correction factor of the target material and calculated from (1). The mass absorption coefficients of incident photons and emitted K_i , μ_{inc} , and μ_{K_i} are given in Table I.

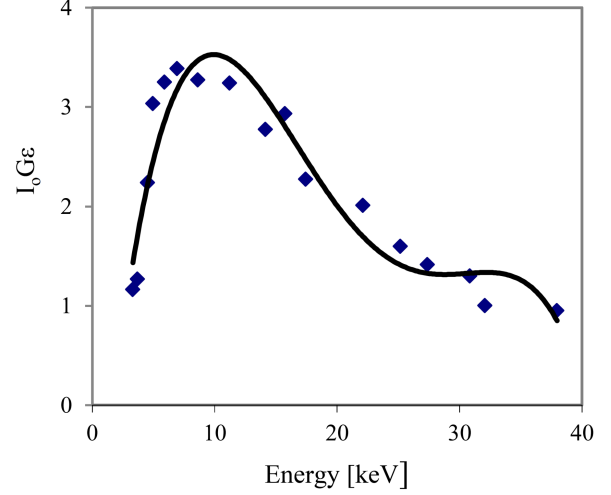


Fig. 2. The detector efficiency $I_0 G \varepsilon_{K_i}$ averages for K_i ($i = \alpha, \beta$) in function of X-ray energy [keV].

TABLE I

Mass absorption coefficients: $\mu_{\text{inc}}, \mu_{K_i}$ [cm^2/g] (where $i = \alpha, \beta$) and sample thickness t [g/cm^2].

Samples	μ_{inc}	μ_{K_α}	μ_{K_β}	t
Ba	8.686	8.291	5.865	0.037
BaF ₂	6.845	6.658	4.664	0.033
Ba(ClO ₃) ₂	4.085	4.320	3.068	0.018
BaCl ₂	5.880	6.155	4.350	0.024
BaSO ₄	5.220	5.214	3.700	0.022
BaO	7.800	7.461	5.283	0.016
Ba(OH) ₂	7.001	6.713	4.758	0.005
Ba(NO ₃) ₂	4.654	4.512	3.214	0.016
BaCO ₃	6.102	5.867	4.165	0.030

The experimental X-ray intensity ratios I_{K_j}/I_{K_i} ($j = \beta_1, \beta_2, i = \alpha_1, \alpha_2$) were evaluated using [22]

$$\frac{I_{K_j}}{I_{K_i}} = \left(\frac{N_{K_j}}{N_{K_i}} \right) \left(\frac{\beta_{K_i}}{\beta_{K_j}} \right) \left(\frac{\varepsilon_{K_i}}{\varepsilon_{K_j}} \right), \quad (7)$$

where (N_{K_j}/N_{K_i}) is the ratio of counting rates under the peaks K_j and K_i , $(\beta_{K_i}/\beta_{K_j})$ is the ratio of the self-absorption correction factor of the target, and $(\varepsilon_{K_i}/\varepsilon_{K_j})$ is the ratio of the detector efficiency values for K_i and K_j X-rays, respectively.

The semi-empirical K shell fluorescence yield ω_K was determined using [2]

$$\omega_K = \frac{\sigma_{\text{tot}}}{\sigma_K(E)}, \quad (8)$$

where σ_{tot} represents the total K X-ray fluorescence cross-section obtained experimentally, and $\sigma_K(E)$ is the K -shell photoionization cross-section taken from tables published by Scofield [19].

TABLE II

Experimental and theoretical K_i ($i = \alpha, \beta$) X-ray fluorescence cross-section [cm^2/g] values.

Samples	σ_{K_α}		σ_{K_β}		σ_{tot}	
	Exper.	Theor.	Exper.	Theor.	Exper.	Theor.
Ba	5.128 ± 0.214	5.163	1.139 ± 0.046	1.172	6.267 ± 0.250	6.203
BaF ₂	5.549 ± 0.236		1.374 ± 0.055		6.923 ± 0.284	
Ba(ClO ₃) ₂	5.490 ± 0.225		1.348 ± 0.057		6.838 ± 0.287	
BaCl ₂	5.481 ± 0.229		1.342 ± 0.060		6.823 ± 0.274	
BaSO ₄	5.416 ± 0.217		1.303 ± 0.052		6.719 ± 0.289	
BaO	5.379 ± 0.215		1.290 ± 0.053		6.668 ± 0.274	
Ba(OH) ₂	5.378 ± 0.217		1.283 ± 0.055		6.662 ± 0.267	
Ba(NO ₃) ₂	5.356 ± 0.214		1.278 ± 0.051		6.634 ± 0.271	
BaCO ₃	5.310 ± 0.211		1.276 ± 0.054		6.586 ± 0.277	

3.3. Determination of K to L shell vacancy transfer probability and Auger electrons emission ratio

Ratios of emission probabilities of Auger electrons ($u=p(KLX)/p(KLL)$, $\nu=p(KXY)/p(KLL)$) were determined using following equations described in detail by Schönfeld and Janßen [23], i.e.,

$$x = \frac{I_{K_\beta}}{I_{K_\alpha}} = \frac{\sigma_{K_\beta}}{\sigma_{K_\alpha}}, \quad (9)$$

$$\nu = \frac{p(KXY)}{p(KLL)} = x^2, \quad (10)$$

$$u = \frac{p(KLX)}{p(KLL)} = 2x. \quad (11)$$

In (9)–(11), X and Y define M, N, O, \dots shell electrons. As seen in (10) and (11), the characterization of Auger electrons is expressed by terminology with three letters. Each letter has a different meaning. The initial vacancy is defined by the first letter. The second letter represents the shell from which an electron fills initial vacancy. The third letter represents the ejected Auger electron shell. For example, the KLM Auger electron is an electron ejected from the M shell when a K shell vacancy is filled by an L electron [2]. The vacancy transfer coefficient η_{KL} describes the mean number of vacancies produced in the L shell by one vacancy in the K shell. If all radiative and nonradiative processes and the production of two vacancies in the L shell by the ejection of the KLL Auger electrons are taken into account, the quantity η_{KL} is given by

$$\eta_{KL} = \frac{2 - \omega_K}{1 + x}. \quad (12)$$

4. Results and discussion

Fluorescence cross-sections ($\sigma_{K_\alpha}, \sigma_{K_\beta}, \sigma_{tot}$), K_β/K_α X-ray intensity ratios, vacancy transfer probabilities from K to L shell (η_{KL}), and ratios of emission probabilities of Auger electrons

($u = p(KLX)/p(KLL)$, $\nu = p(KXY)/p(KLL)$) for pure Ba and BaF₂, Ba(ClO₃)₂, BaCl₂, BaSO₄, BaO, Ba(OH)₂, Ba(NO₃)₂, BaCO₃ compounds were studied using K_i X-rays line intensities (where $i = \alpha, \beta$). The overall error in the present measurement is estimated to be $\approx 5\%$. This uncertainty was attributed to the uncertainty of the photon intensities ($\leq 3\%$), detector efficiency ($\leq 3\%$), mass per unit area of samples ($\leq 1\%$) and the self-absorption correction factor ($\leq 1\%$) in the measurements.

The uncertainties of cross-section were determined according to the expression [2, 24]

$$\text{Uncert.} = \left(\frac{\Delta\beta}{\beta}\right)^2 + (\text{exp. results})$$

$$\times \sqrt{\left(\frac{\Delta N}{N}\right)^2 + \left(\frac{\Delta I_0 G \varepsilon}{I_0 G \varepsilon}\right)^2 + \left(\frac{\Delta t}{t}\right)^2}, \quad (13)$$

where ΔN represents the uncertainty of counts rate under the photo peak, N is the number of counts rate under the photo peak, $I_0 G \varepsilon$ represents the detector efficiency, $\Delta I_0 G \varepsilon$ is the uncertainty in $I_0 G \varepsilon$, t is the mass thickness of the sample, Δt represents the uncertainty of mass thickness, β is the self-absorption correction factor and $\Delta\beta$ represents the uncertainty of the self-absorption correction factor.

The experimental K_α , K_β X-ray fluorescence cross-sections and the total K -shell X-ray fluorescence cross-section were determined using (6). The experimental K shell X-ray fluorescence cross-section values are given in Table II with calculated fluorescence cross-section from (3). Differences between experimental results obtained from the barium compounds and pure Ba for σ_{K_α} , σ_{K_β} and $\sigma_{K_{tot}}$ X-ray fluorescence cross-sections are $\leq 4\text{--}8\%$, $12\text{--}21\%$, $6\text{--}10\%$, respectively. Also, it was found the differences between the experimental results and the calculated theoretical values for the same parameters are $3\text{--}7\%$, $9\text{--}18\%$ and $9\text{--}11\%$, respectively.

TABLE III

Experimental and theoretical X-ray intensity ratio, X-ray fluorescence yield and K to L shell vacancy transfer probabilities (η_{KL}) values.

Samples	K_{β}/K_{α}		ω_K		η_{KL}	
	Exper.	Other	Exper.	Other	Exper.	Other
Ba	0.222 ± 0.013	0.227 [21] 0.236 [25] 0.227 [26] 0.235 [27]	0.892 ± 0.053	0.902 [20] 0.899 [26] 0.89214 [28]	0.907 ± 0.054	0.890 [25] 0.887 [29] 0.905 [30] 0.882 [31]
BaF ₂	0.248 ± 0.014		0.985 ± 0.059		0.813 ± 0.049	
Ba(ClO ₃) ₂	0.246 ± 0.015		0.973 ± 0.058		0.824 ± 0.049	
BaCl ₂	0.245 ± 0.014		0.971 ± 0.058		0.826 ± 0.049	
BaSO ₄	0.241 ± 0.014		0.956 ± 0.057		0.841 ± 0.050	
BaO	0.240 ± 0.014		0.949 ± 0.057		0.848 ± 0.051	
Ba(OH) ₂	0.239 ± 0.014		0.948 ± 0.057		0.849 ± 0.051	
Ba(NO ₃) ₂	0.239 ± 0.014		0.944 ± 0.057		0.852 ± 0.051	
BaCO ₃	0.240 ± 0.014		0.938 ± 0.056		0.857 ± 0.051	

The experimental K X-ray intensity ratios, $I_{K_{\beta}}/I_{K_{\alpha}}$, were compared with the theoretical values (Scofield, 1974) and other experimental values [25–27], see Table III. It can be seen that the differences between experimental values for the Ba compounds relative to pure Ba are in the range of 8–12%. Also, it is determined that the experimental K X-ray intensity ratios agree with the theoretical prediction from Scofield (1974) within range of 6–9% and the differences between the present and other experimental values of the intensity ratios ($I_{K_{\beta}}/I_{K_{\alpha}}$) are within range \sim 2–9%.

The experimental K shell fluorescence yields (ω_K) and the experimental K X-ray fluorescence cross-sections were determined using (6). The experimental values of the K shell fluorescence yields were compared to other experimental [26] and theoretical [20, 28] values in Table III.

Empirical K shell fluorescence yields (ω_K) from the available experimental data for elements with $6 \leq Z \leq 99$ were calculated by Kahoul et al. [28]. A comparison is made between the results of the procedures and the literature theoretical and empirical values. It is seen that the calculated values for Ba agree with our experimental values for pure Ba. Also, the differences between our experimental values for pure Ba and other experimental [26] and theoretical values were determined to be 0.78–1.12%. Changes of experimental values with respect to pure Ba are in the range 5–11%.

The values of the K to L shell vacancy transfer probabilities (η_{KL}) are given in Table III with other experimental and theoretical values [25, 29–31]. The differences between the experimental values relative to the pure Ba of the K to L shell vacancy transfer probabilities (η_{KL}) are \sim 6–11%. The agreement between the present results and other experimental

and theoretical values of the K to L shell vacancy transfer probabilities are found to be 4–8%, 4–8%, 6–11%, 3–9%.

Finally, the Auger electrons emission ratios (u, ν) were obtained by (10) for KLX/KLL and (11) for KXY/KLL using experimental intensity ratios for elements and compounds. In Table IV the Auger electrons emission ratios are given with theoretical calculation and other experimental and theoretical results. The agreement between the experimental values of the $u = KLX/KLL$ Auger electrons emission ratios are within \sim 7–12%. We also note that the experimental $\nu = KXY/KLL$ Auger electrons emission ratios agree with the theoretical predictions in the range 16–25% range.

As can be seen from the experimental values, K X-ray parameters are affected by the chemical structure of the sample. It is observed that the chemical effect on the K_{β} and ($I_{K_{\beta}}/I_{K_{\alpha}}$) intensity ratios and KXY/KLL (ν) Auger electrons emission ratios is remarkable. The reason for this is that the transitions occur in the valance shell or the shells near to the valance shell.^{†1} It is a well-known fact that the orbital energy levels of L, M, N and O shells get closer to each other as the quantum number n increases, and outer energy levels become sensitive to the chemical environment. Thus, according to the crystal field theory, the outer energy levels are more strongly affected by ligands.

When an atom takes part in a chemical bonding, the valance atomic orbitals participate in the formation of molecular orbitals of the compounds.

^{†1}The origin of K_{β} X-ray is electron transitions from the M and N shells to K shell.

TABLE IV

Auger electrons emission ratios for Ba compounds.

Samples	$u = p(KLX)/p(KLL)$		$v = p(KXY)/p(KLL)$	
	Exper.	Other	Exper.	Other
Ba	0.444 ± 0.026	0.477 [23] 0.472 [25]	0.049 ± 0.003	0.057 [23] 0.472 [25]
BaF ₂	0.495 ± 0.030		0.061 ± 0.004	
Ba(ClO ₃) ₂	0.491 ± 0.029		0.060 ± 0.004	
BaCl ₂	0.490 ± 0.028		0.060 ± 0.004	
BaSO ₄	0.481 ± 0.029		0.058 ± 0.004	
BaO	0.479 ± 0.029		0.057 ± 0.004	
Ba(OH) ₂	0.477 ± 0.029		0.057 ± 0.004	
Ba(NO ₃) ₂	0.477 ± 0.029		0.057 ± 0.004	
BaCO ₃	0.480 ± 0.029		0.058 ± 0.004	

The structures of these molecular orbitals are determined by the nature of the component atoms in the bond. When creating molecular structures, valance electrons are either transferred from an atom or shared as electron pair between compound atoms. This process depends on the electron affinity and electronegativity of the atom. The atom having the largest electronegativity more strongly attracts the electrons of its component atoms. Therefore, the atoms in a compound change the order of the electrons. According to our results, F and Cl are halogen and possess a higher value of electron affinity and electronegativity with respect to the other atoms in the compounds investigated in this study. Thus, F and Cl strongly influence outer shell electrons (or valance electrons) of the component atoms in their compounds.

The chemical bonding type (ionic, metallic, and covalent) and the bond length affect the K shell fluorescence parameters. According to the molecular orbital theory, molecular orbitals get closer to the nucleus as the interatomic distance increases. The approach towards the nucleus leads to higher electron bond energies. The valance state of the atom has a profound effect on lineshapes and related parameters of spectra, such as the Auger event and relative intensity. Valance electrons that participate in the formation of chemical bonds are removed from the atom, and this effect causes a change in the electronic screening and a change in outer shell binding energies. These variations affect the life time of the state, and therefore the intensity and lineshapes of the characteristic X-ray are modified. The change of the intensity and the shape of the peak strongly affect the radiative and non-radiative transitions probabilities. For this reason, the ratios of emission probabilities of Auger electrons ($u = p(KLX)/p(KLL)$, $v = p(KXY)/p(KLL)$) are affected by the chemical environment of the emitting atoms and a more remarkable change was observed in the Auger parameters compared to others.

5. Conclusions

Some K X-ray parameters for Ba compounds were studied using the K_i ($i = \alpha, \beta$) X-rays line intensities. The experimental results were compared with other theoretical and experimental values of Ba element. According to the results, when the measured value for the compounds and those for pure Ba are compared, the percentage changes in experimental values were determined. In particular, it was observed that the chemical effect was more dominant in the X-ray parameters measured for K_β X-rays. These changes shows that the X-ray parameters are affected by the chemical structure. Factors such as the type of bond, the bond lengths, the state of the valance electrons, the oxidation number play a role in the formation of the chemical effect.

For the experimental K-shell X-ray fluorescence cross-sections, it was observed in the studied Ba compounds that the chemical effect was higher in F and Cl compounds, and the F and Cl compounds were more affected by the chemical structure. As a reason for this result, it can be said that F and Cl have high affinity and electronegativity values. During bond formation, these values affect the valance electron population and the electron arrangement of atom, and this rearrangement in the atomic structure influences the characteristic X-rays emitting from the atomic levels. Thus, it is seen that affinity and electronegativity values are one of the most important parameter for the chemical effect.

References

- [1] M. Doğan, E. Cengiz, G. Dilber, A. Nas, E. Tıraşoğlu, H. Kantekin, *Radiat. Phys. Chem.* **101**, 30 (2014).
- [2] M.F. Turhan, A. Turşucu, F. Akman, F. Akdemir, R. Durak, *Radiat. Phys. Chem.* **168**, 108564 (2020).
- [3] M. Ugurlu, L. Demir, *Spectrosc. Lett.* **53**, 63 (2020).

- [4] R. Kumar, A. Rani, R.M. Singh, M.K. Tiwari, *Radiat. Phys. Chems.* **156**, 283 (2019).
- [5] F. Akman, *Appl. Radiat. Isot* **115**, 295 (2016).
- [6] F. Akman, *Can. J. Phys.* **94**, 679 (2016).
- [7] L.F.M. Anand, S.B. Gudennavar, S.G. Bubbly, B.R. Kerur, *J. Exp. Theo. Phys.* **121**, 961 (2015).
- [8] S. Mirji, A.S. Bennal, N.M. Badiger, M.K. Tiwari, G.S. Lodha, *Chem. Phys. Lett.* **634**, 271 (2015).
- [9] M. Doğan, E. Cengiz, A. Nas, E. Tıraşoğlu, H. Kantekin, V. Aylıkçı, *Appl. Radiat. Isot.* **104**, 43 (2015).
- [10] L.F.M. Anand, S.B. Gudennavar, S.G. Bubbly, B.R. Kerur, *J. Exp. Theo. Phys.* **119**, 392 (2014).
- [11] A. Turşucu, D. Demir, *Appl. Radiat. Isot.* **77**, 23 (2013).
- [12] A. Tursucu, P. Onder, M. Eroglu, D. Demir, *Appl. Radiat. Isot.* **70**, 1509 (2012).
- [13] G. Apaydin, E. Tirasoglu, *Radiat. Phys. Chem.* **81**, 1593 (2012).
- [14] B.G. Durdu, A. Kucukonder, *Radiat. Phys. Chem.* **96**, 140 (2014).
- [15] B.G. Durdu, *Can. J. Phys.* **96**, 202 (2018).
- [16] A. Kucukonder, B.G. Durdu, *Chem. Phys. Lett.* **579**, 132 (2013).
- [17] *PubChem database* at the National Institutes of Health (NIH), 2020.
- [18] L. Gerward, N. Guilbert, K.B. Jensen, H. Levring, *Radial. Phys. Chem.* **71**, 653 (2004).
- [19] J.H. Scofield, M.Sc. Thesis, Lawrence Livermore Laboratory, 1973.
- [20] M.O. Krause, *J. Phys. Chem. Ref. Data* **8**, 307 (1979).
- [21] J.H. Scofield, *Atom. Data Nucl. Data Table* **14**, 121 (1974).
- [22] E. Cengiz, O.K. Köksal, G. Apaydın, İ.H. Karahan, E. Ünal, *Appl. Radiat. Isot.* **144**, 24 (2019).
- [23] E. Schönfeld, H. Janßen, *Nucl. Instrum. Meth.* **A369**, 527 (1996).
- [24] F. Akman, R. Durak, M.R. Kaçal, M.F. Turhan, *Can. J. Phys.* **93**, 1057 (2015).
- [25] E. Baydaş, *Instrum. Sci. Technol.* **33**, 461 (2005).
- [26] I. Han, M. Şahin, L. Demir, Y. Şahin, *Appl. Radiat. Isot.* **65**, 669 (2007).
- [27] M. Ertuğrul, Ö. Söğüt, Ö. Şimşek, E. Büyükkasap, *J. Phys. B. At. Mol. Opt. Phys.* **34**, 909 (2001).
- [28] A. Kahoul, A. Abassi, B. Deghfel, M. Nekkab, *Radial. Phys. Chem.* **80**, 369 (2011).
- [29] P.V. Rao, M.H. Chen, B. Crasemann, *Phys. Rev. A* **5**, 997 (1972).
- [30] B. Ertuğral, G. Apaydın, A. Tekbıyık, E. Tıraşoğlu, U. Çevik, A.İ. Kobya, M. Ertuğrul, *Eur. Phys. J. D* **37**, 371 (2006).
- [31] B. Ertugral, U. Cevik, E. Tirasoglu, M. Ertugrul, O. Dogan, *J. Quant. Spectrosc. Radiat. Transfer* **78**, 163 (2003).